A00-16423

AIAA 2000-0546

Numerical Simulation of Micromachined Acoustic Resonators

Robert P. Moran, Peter D. Washabaugh
Michael O. Müller, Luis P. Bernal
Department of Aerospace Engineering

Babak Amir Parviz, Khalil Najafi
Department of Electrical Engineering and Computer Sciences

University of Michigan
Ann Arbor, MI 48109-2140

38th Aerospace Sciences Meeting & Exhibit
10-13 January 2000 / Reno, NV

AIAA-2000-0546

NUMERICAL SIMULATION OF MICROMACHINED ACOUSTIC RESONATORS

Robert P. Moran§, Peter D. Washabaugh*, Luis P. Bernal*, Michael O. Müller§,
Department of Aerospace Engineering

Babak Amir Parviz†, Khalil Najafi‡
Department of Electrical Engineering and Computer Science

University of Michigan
Ann Arbor, Michigan 48109-2140

ABSTRACT

An acoustic resonator coupled with an ejector shroud is being studied as a suitable propulsion system for Micro Airborne Vehicles (MAV's). The acoustic resonator uses an electrostatically actuated vibrating diaphragm to create an acoustic wave that is amplified in a resonator cavity and focused in an adjoining nozzle to produce acoustic streaming. Multiple resonators placed along the periphery of an ejector will enhance mass flow and provide thrust to act as the propulsion system for a micro airborne platform (MAP). A special feature of this design is that a large array can be fabricated using inexpensive Micro Electro Mechanical Systems (MEMS) technology. A prototype MEMS propulsion device and a 10:1 scale device have been constructed. A computational fluid dynamics (CFD) model of the 10:1 device has been developed. This paper reports on these numerical simulations.

The CFD simulation models the diaphragm motion in a frequency range of .5 to 8.5 kHz. The diaphragm shape is assumed to be a half sinusoid in two directions and have a deflection amplitude of 60μm peak to peak at the center. When the model is compared with the 10:1 device. The numerical model appears to accurately predict the resonant frequencies of the system.

INTRODUCTION

A significant difficulty of achieving flight with Micro Airborne Vehicles (MAV's) is the lack of an adequate micro propulsion system that is simultaneously efficient and economical to fabricate. A novel device that may provide a solution to both of these problems is an acoustic resonator coupled with an ejector shroud. The acoustic resonator uses an electrostatically actuated vibrating diaphragm to create an acoustic wave. The wave is amplified in a resonator cavity and focused in an adjoining nozzle to produce an acoustic stream or micro jet of air[1] A cross-section of such a resonator design is shown in figure 1.

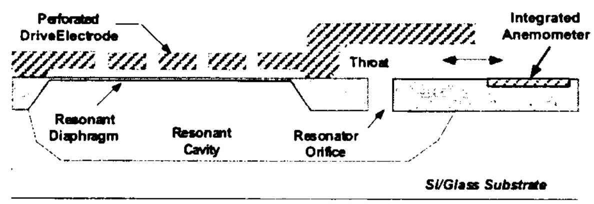

Figure 1: Schematic of an acoustic resonator.

Multiple resonators placed along the periphery of an ejector will enhance mass flow and could theoretically provide sufficient thrust to act as the primary propulsion system for a micro airborne platform (MAP). This micromachined acoustic ejector (MACE), will consist of four or more acoustic resonators, a diffuser shaped inlet, and a diverging nozzle outlet. The ejector shroud will entrain air at the expense of flow velocity. There will be an accompanying increase in mass flow and thereby thrust. A cross-section of a proposed MACE is shown in figure 2.

The MEMS fabricated resonators are simple, lightweight, solid state electronic pumps. Because of the shape of the nozzle an overall net resistance is encountered by incoming air, and a net thrust is created in the favored outgoing direction during each vibration cycle. A prototype of a MEMS manufactured resonator is shown in figure 3.

This full-scale device has a membrane actuator that is 1.2mm square and 6μm thick. The membrane is a composite that is composed of layers of SiO_2, SiNi, and p^{++} doped Si[2] This composite structure is necessary to control the in-plane stress in the membrane and to

§ Graduate Research Assistant, Department of Aerospace Engineering, Member AIAA.
* Associate Professor, Department of Aerospace Engineering, Senior Member AIAA.
† Graduate Research Assistant, Department of Electrical Engineering and Computer Science.
‡ Professor, Department of Electrical Engineering and Computer Science.

provide an insulating surface. This electrode is separated from the membrane by a distance of 3μm. The perforations in the electrode are necessary to reduce air damping of the membrane motion.

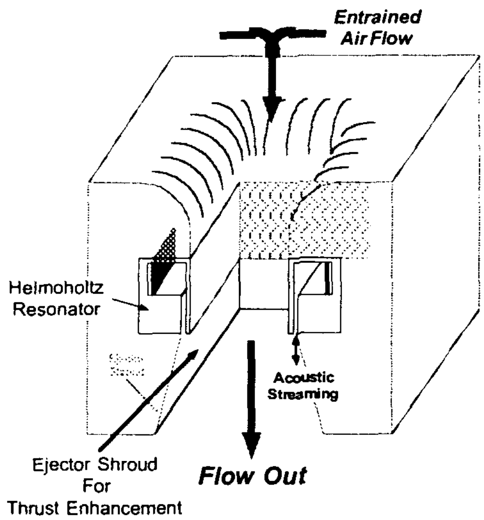

Figure 2: Schematic of a micromachined acoustic ejector (MACE).

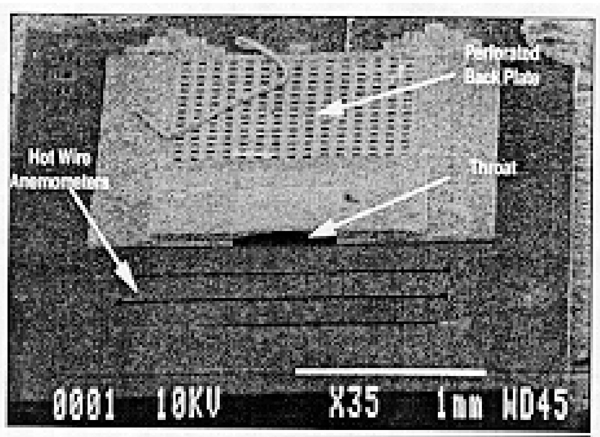

Figure 3: Scanning electron microscope image of a full scale MEMS fabricated resonator.

The full scale membrane is under a tensile stress that can be as high as 100 Mpa. The membrane is pulled toward the electrode by an electric charge and when the charge is removed the elasticity of the structure causes the system to spring back toward its initial position. As the charge is varied, the membrane will vibrate and thereby excite acoustic modes in the cavity. In the full scale device the electric field on the membrane is sufficient to collapse it against the drive electrode[3]. This is done to achieve the largest possible volume change for a given geometry.

When the diaphragm compresses the working fluid, in this case air, a high-pressure wave is created within the cavity. The resonator cavity and nozzle have an acoustic wavelength that is associated with the geometric dimensions of the cavity and the throat, as well as the compressibility of the working fluid. The full scale resonator pictured in figure 3 has an approximate cavity volume of $0.58mm^3$. The nozzle throat is 30μm high, by 150μm wide and 550μm long. The cavity is approximately 140 μm high, by 1200 μm wide, by 2400 μm long with the irregular shape shown in figure 1.

An analytic reduced order acoustic theory predicts that by resonating the diaphragm at its first resonant frequency and by matching this frequency to the natural frequency of the cavity enclosure a significantly enhanced velocity (acoustic streaming), mass flow, and momentum will be obtained at the nozzle[4]. A significant design driver is the matching or close coupling of the structural and fluidic natural frequencies. Impedance matching of the drive electronics may also be an issue in term of overall system efficiency.

This full-scale device is intended to operate at voltages up to 300V, and frequencies greater than 50kHz. The voltages are kept relatively low in order to simplify the drive electronics, and the frequency of the diaphragm is kept high to create a large Reynolds number (Re>10) in the throat. The high frequency has the additional bonus of reducing the audible acoustic signature of the device.

To help substantiate the analytical model, to understand the system performance, and to assist in the design, a series of numerical models were created. These models simulate aspects of the diaphragm motion and the resulting flow within the resonator cavity. The models were written in the commercially available CFD code, Fluent.[5] The models should accurately predict the time-dependant acoustic pressure field created inside the resonator. The most general model currently incorporates compressibility, an assumed diaphragm motion, and viscous effects in two dimensions. A less complex three dimensional model has also been implemented.

The CFD model was substantiated by comparison with simple pipe acoustics[6] and a one-dimensional compressible model[4]. Aspects of the model have been verified with a 10:1 geometrically scaled experiment. Currently the 10:1 scaled device has been studied in some detail using a two dimensional numerical model. The numerical model predicts the first cavity mode and provides insight into the internal flow of the resonator cavity.

NUMERICAL MODELS

The computational models to simulate the 10:1 geometrically scaled resonator were developed in an incremental approach in which an initial simple model was slowly increased in complexity. Model improvements focused on capturing significant physical effects. Important features of the models are described below.

An Incompressible Model

The initial numerical study focused solely on accurately describing the deformation of the membrane as it moved in its first mode. The fluid was modeled as incompressible. Modeling the motion of the boundary required that two nearly identical grid geometries be described. Each grid was comprised of approximately 10,000 cells. The first grid described the shape of the membrane in its initial maximum concave position at t = 0. This initial position assumed that the membrane had been pulled toward the electrode by the electromagnetic forces and was in a half-sinusoidal shape. The second grid had exactly the same number of computational cells but with some compression of the cells in the vicinity of the membrane. This second grid described the shape of the membrane when it had reached its full deflection in the convex position. The maximum convex deflection of the actual device is dependent on the material properties of the membrane, the tension applied to it, and its interaction with the fluid. This shape was also assumed to be a half-sinusoid.

It is important to note that the deforming domain in these simulations have a constant number of control volumes. These volumes are simply distorted as a prescribed function of time. Care must be taken to keep reasonable aspect ratios of the mesh throughout the time cycle. Also, since the shape is prescribed there is no fluid-structure interaction that changes the shape of the boundary.

This incompressible numerical study simulated the system at the expected maximum frequency of 8.5kHz and numerically approximates the Euler equations.[5] This frequency resulted in a maximum velocity of the membrane, at the center, of +/-1 m/s. Through one complete cycle, in order to clearly capture the internal flow and its reversal, 10 time steps were taken. The flow predicted from this numerical model agreed with the incompressible 1-dimensional model[4].

Compressible Modeling

Acoustic streaming is a phenomenon that is due to compressibility of the fluid. However, incorporating compressibility effects into the CFD model was not straightforward. Simply using the incompressible mesh and solution parameters to approximate the Navier-Stokes equations proved to give poor results that usually did not converge. Fluent uses a finite difference semi-implicit pressure line relaxation scheme of Patankar.[5] The initial compressible simulations had unrealistic velocities through out the flow field and did not achieve mass balance (in and out of the throat) during a cycle.

Various steps were taken to get the simulation to give more reasonable results. For instance an early compressible model broke the initial simulation into a sequence of compression and expansion half cycles. This half-cycle division was taken to further study the effect on the model of flow reversal in the vicinity of the throat. Here the flow field results from one half-cycle was fed as initial conditions to the next cycle. Breaking the model into these smaller steps allowed parameters such as the time steps, iterations, and error residuals to be modified and thereby provide insight into the behavior of the system. However, varying solution parameters during a simulation calls into question the robustness and the validity of the entire solution procedure. The approach that was ultimately found to be useful was quite simple.

To get consistent results from the compressible model the spatial grid was left alone, but the number of time steps for each cycle was set at 40, with the maximum number of iterations to satisfy the balance principles being set to 100. In addition the error residuals in this balance, particularly for pressure, was reduce by a few percent. Finally in order to achieve mass balance of the flow in and out of the cavity from the initial quiescent conditions, the simulation needed to run for 8 full cycles.

The simulation was run for a cycle with the results of the previous cycle being fed into the next cycle as initial conditions. With each cycle the pressure wave became more pronounced and a greater amount of the mass leaving the nozzle would return. After eight cycles the model was mass balanced with as much mass leaving the nozzle during the expansion half of the cycle as was returning during the compression half of the cycle. The results reported here are from this compressible model solution procedure.

At the initial model frequency of 8.33 kHz a standing wave formed within the cavity. This wave pattern put the nozzle 90 degrees out of phase with the membrane motion. This means that air streams out of the nozzle during the membrane expansion half of the cycle, and back in through the nozzle during the compression half of the cycle. A further refinement of the time steps to 120 per cycle clearly showed the standing wave pattern. Simple hand calculations of wavelength showed that the 8.33 kHz was very close to the acoustic cavities second frequency mode. This result along with the balanced mass flux were key requirements for proof that the computational model was indeed radiating an acoustic pressure wave. Further results are described below.

Compressible Model Results

The geometry analyzed was identical to the 10:1 scaled device described earlier (150 μm x 10 = 1.5 mm long nozzle). A second model of nearly identical geometry was also created in order to investigate trends in varying the throat length. This second model had a throat length of 4 mm.

Spectra

A frequency sweep of the 1.5mm long throat model was performed by changing the membrane center velocity. Nozzle exit velocity and cavity pressure data was obtained in 500 Hz frequency increments from .5 kHz to 8.5 kHz. This comprised a total of 17 different frequency models each running for approximately 8 hours on a Sun Ultra spark 10 for a total of 136 computer hours. The 4mm model was similarly analyzed in parallel.

These numerical results were also compared with results from a simple acoustic duct (closed-closed and open-closed)[6], and a reduced order model ("reduced model")[4]. The duct model is based on cavity length and hydraulic diameter. The acoustic duct model assumes a tubular geometry that is closed at one end and either open or closed at the opposite end. This model does not consider the 2-dimensional varying geometry of the actual cavity, or the constriction of the nozzle exit and is therefor quite limited.

The reduced order model takes into account the time varying volume of the system along with compressibility effects of the working fluid and the flow length as a function of the throat. These results are plotted in figure 4.

The simple acoustic duct model does appear to indicate the rough vicinity of the 2nd natural frequency of the cavity. The reduced order model predicts almost exactly the same 1st mode frequencies for both throat lengths but at slightly higher amplitudes. This is most likely because the reduced order model does not take into account the details of the varying geometry of the cavity which certainly has an affect on flow losses and thereby velocity in the throat.

Pressure Contours

The following three pictures in figure 5 illlustrate the acoustic pressure wave as it moves through the cavity. These images were obtained from the 8.33 kHz model with a 4mm long nozzle. This is the second mode of the cavity. The membrane shape is assumed to be a half-sinusoid, with a center deflection of +/-30μm (60μm peak to peak) at maximum amplitude. Results were obtained from the eighth cycle of the deforming membrane so that transient effects were essentially eliminated. Though the wave does take a finite amount of time to translate from one end of the cavity to the other, it is quite fast in that at this scale it takes only tens of microseconds for the pressure wave to traverse the cavity. To capture the wave for this configuration during its motion through the cavity the time step period was set to 1μs for a total of 120 step in a cycle.

The diaphragm started traveling upward at a time of 340μs. It will finish the upward portion of its stroke at a time of 400μs. The highest pressure in the cavity of , approximately 2 kPa, is at the opposite end from the nozzle and is beneath the diaphragm as shown in figure 5a. Ten microseconds later, Figure 5b shows the pressure pulse after it has passed the mid position of the cavity and as it enters the vicinity of the nozzle. Finally another 10μs later, as shown in figure 5c, the high pressure has almost reached the portion of the cavity away from the diaphragm and directly under the nozzle. The pressure at the nozzle exit is constrained to be at an ambient condition of one atmosphere. The flow velocity during the sequence is generally <u>inward</u> with a magnitude monotonically <u>decreasing</u> from approximately 7 m/s to 0 m/s.

Since figure 5 illustrates the 2nd mode, the motion in the throat is out of phase by 90 degrees with respect to the diaphragm motion. Figure 5c is a snapshot just when the flow in the throat reverses and the high pressure in the vicinity of the nozzle results in an outward velocity.

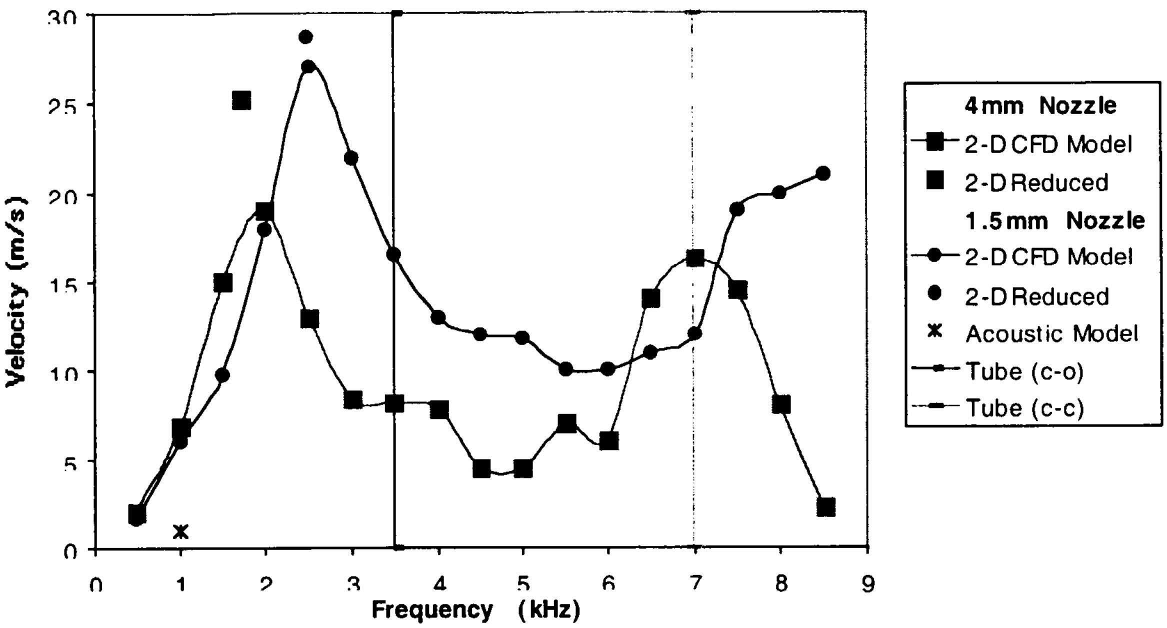

Figure 4: The predicted average nozzle exit velocity as a function of diaphragm excitation frequency from the 2-D Compressible CFD model. In addition a comparison is made between the 2-D compressible CFD model and simple duct acoustic resonant frequencies and a 2-D reduced order model. The membrane is vibrating with a 60μm amplitude peak-to-peak simulating the 10:1 scaled device.

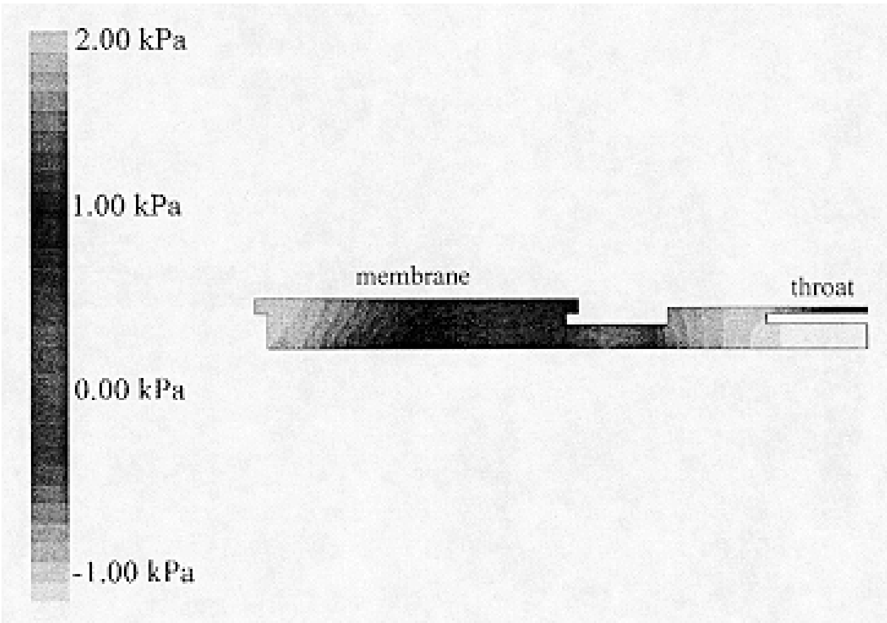

Figure 5a: Pressure contours of the 2[nd] mode in the resonator at a time of 350 μs The highest pressure is in the vicinity of the diaphragm, away from the throat. The flow direction is inward.

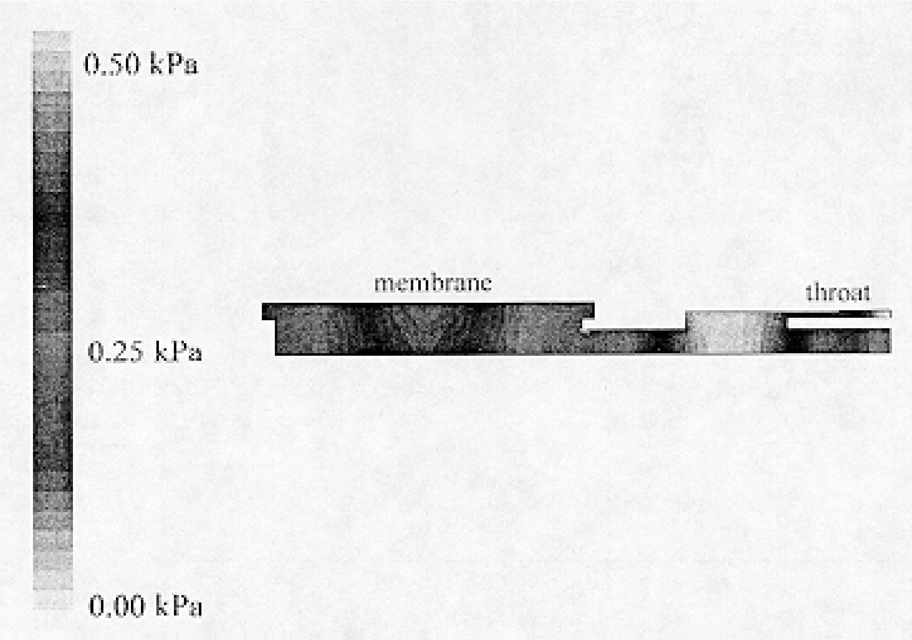

Figure 5b: Pressure contours of the 2[nd] mode in the acoustic resonator at a time of 360 μs. The highest pressure has just moved past the constriction in the cavity, in the vicinity of the nozzle.

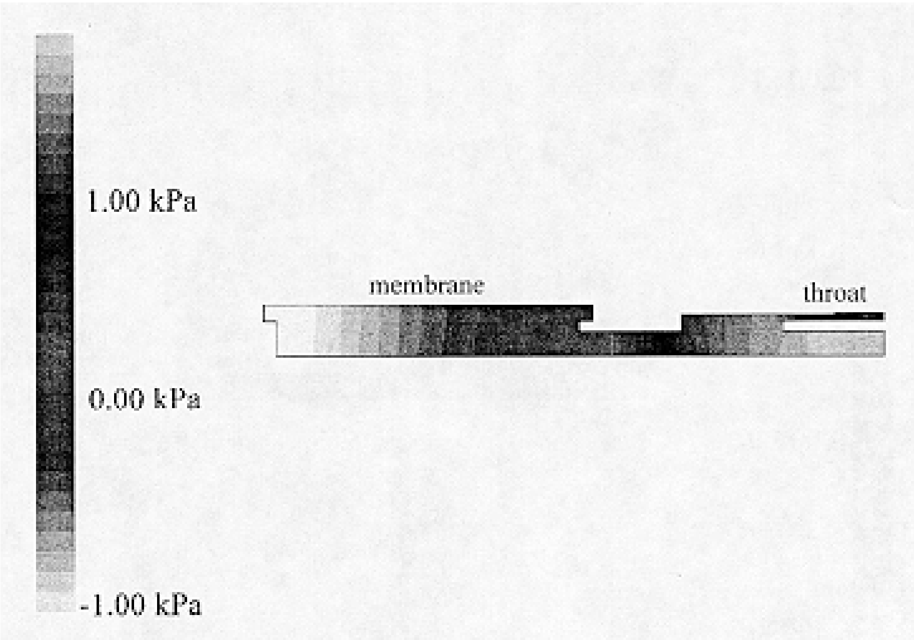

Figure 5c: Pressure contours of the 2[nd] mode in the acoustic resonator at a time of 370 μs. The highest pressure, of approximately 1.5 kPa, is now in the vicinity of the nozzle. The velocity in the throat is approximately zero.

VALIDATION

In order to quickly validate both the CFD simulation and the reduced order model a 10:1 geometrically scaled model was constructed. This device is large enough that typical fluid and solid mechanical testing techniques can more readily employed than on the microscopic MEMS full scale device.

10:1 Experiment

This device is constructed of a series of plates that are bolted together as illustrated in figure 6. This layering superficially mimics how the MEMS device is constructed except on a larger scale, employing different materials and manufacturing techniques. A brass block (1) and brass plate (2) combine to form the main cavity. Brass plates (3) and (4) form the nozzle. The throat is a small indentation in plate (4). An aluminized Mylar diaphragm (not shown) is sandwiched between plates 4 and 5. Plate 5 is made of nylon which acts as an insulator between plate 6 and the rest of the system. Plate 6 is a perforated copper electrode that is ultimately wired to a high voltage amplifier. Plate 7 is also made of nylon and has a machined pocket in which the electrode (6) sits to position and insulate the high voltage from the surroundings. Power is supplied by high voltage wires (not shown) that exit through the front hole in block 8. Plates 1,2,3,4, and 8 are machined, and finished to allow a thin layer of silicone vacuum grease to seal the main cavity. A digital photo of the mounted assembly is shown in figure 7.

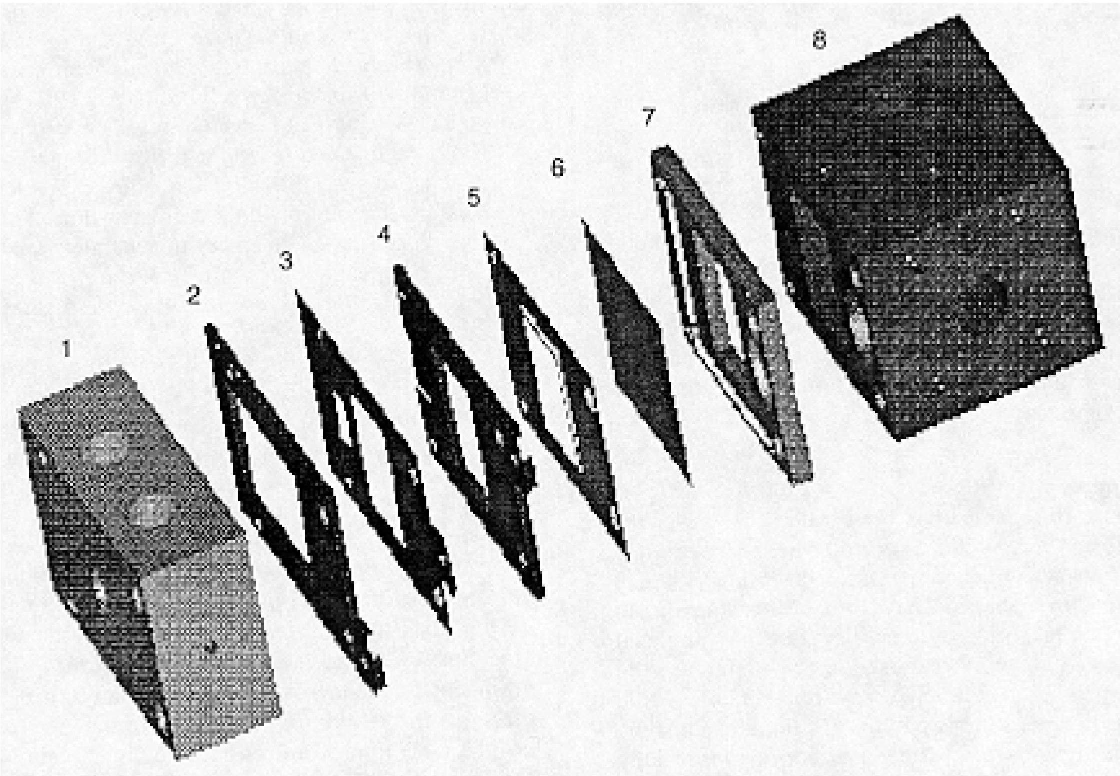

Figure 6: An exploded view of the 10:1 scale model construction.

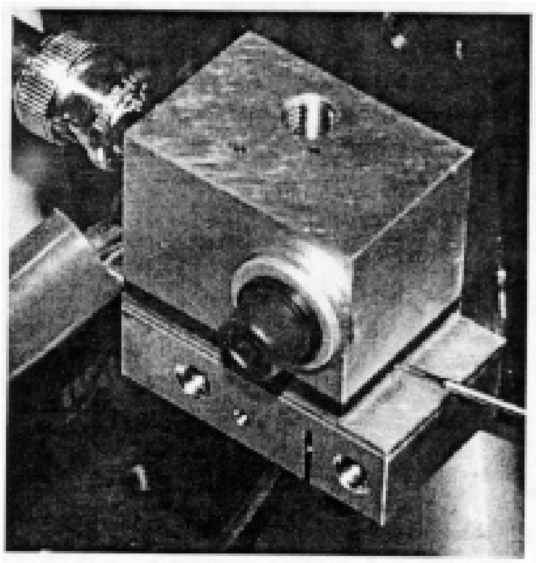

Figure 7: The 10:1 geometric device showing the hotwire anemometer placed in the throat

The flow velocity at the throat is measured with a hot wire anemometer, simultaneously the diaphragm position is measured with a fiber optic probe. The hot wire anemometer has a 5μm diameter. The position sensor measures the defection of the diaphragm, at the center. The hot wire is also shown in figure 7 however the fiber optic position sensor comes up from the bottom and is obscured from view.

Preliminary Results

The 10:1 device has been tested. However the results are very preliminary in the sense that certain actuation performance measures that were assumed in the above analysis have not been achieved. In some cases the problems have been somewhat challenging to diagnose. For instance the performance of the electrostatic actuator would evolve in time. It turns out that the aluminum coating on the mylar would oxidize and corrode (especially in the presence of excessive humidity) and thereby loose its electrical conductivity. This has recently been resolved by coating the membrane with 1000 to 4000 angstrom thick layers of aluminum and de-humidifying the test environment. In order to diagnose some of these issues the spectrum of the membrane was characterized by placing the entire apparatus in a vacuum chamber to remove the effects of almost all fluid-structure interactions.

There is also recent evidence that suggests that characterizing the membrane with a single centrally placed displacement sensor is not sufficient. The membrane appears to be deflecting asymmetrically in simple static tests. This may be due to lack of uniformity in the tensioning stress, or the separation between the membrane and the electrode. This asymmetry would effect the volume displaced in the cavity and thus the magnitude of the velocity in the throat. Even with some of these difficulties the membrane has been oscillated with a +/-14μm deflection and flow velocities of greater than 1 m/s have been measured.

Nevertheless even with these reservations some features of the experiment can be compared with the analyses. Figure 8 shows the predicted and measured velocities. The 10:1 experiment provides diaphragm deflection, and velocity data between .5 kHz and 8.5 kHz. The measured resonant frequency, and the general shape of the graph are consistent with the predictions. The CFD model and the 10:1 scaled device closely agree in terms of resonant frequencies for both the first and second mode of the main cavity. The fact that the CFD model is able to predict the resonant frequency of this irregularly shaped actual device demonstrates its ability to accurately simulate the time-dependant acoustic pressure wave that moves throughout the resonant cavity and adjoining nozzle.

However, the measured velocities deviate significantly from the predicted values by at least two orders of magnitude. This may be partially accounted for in that the work input for the synthetic jet in this configuration is an electrostatically driven membrane. The shape of the membrane under load is questionable.

More importantly the peak to peak membrane deflection in figure 8 was considerably less than the 60μm peak to peak deflection that was assumed in the models. The membrane deflection at the 2.4 kHz resonant frequency of the cavity is only 1μm. The fact that the membrane deflection is only one sixtieth of the CFD model deflection partially explains why the velocities of the model and 10:1 device differ by approximately a factor of 100.

Current efforts are focussing on resolving this discrepancy in velocity. The CFD model has been re-evaluated using the measured deflection from the experiment. Further calibration of the diaphragm deflection, and shape is needed to better emulate the 10:1 device. One result from this effort is shown in figure 9.

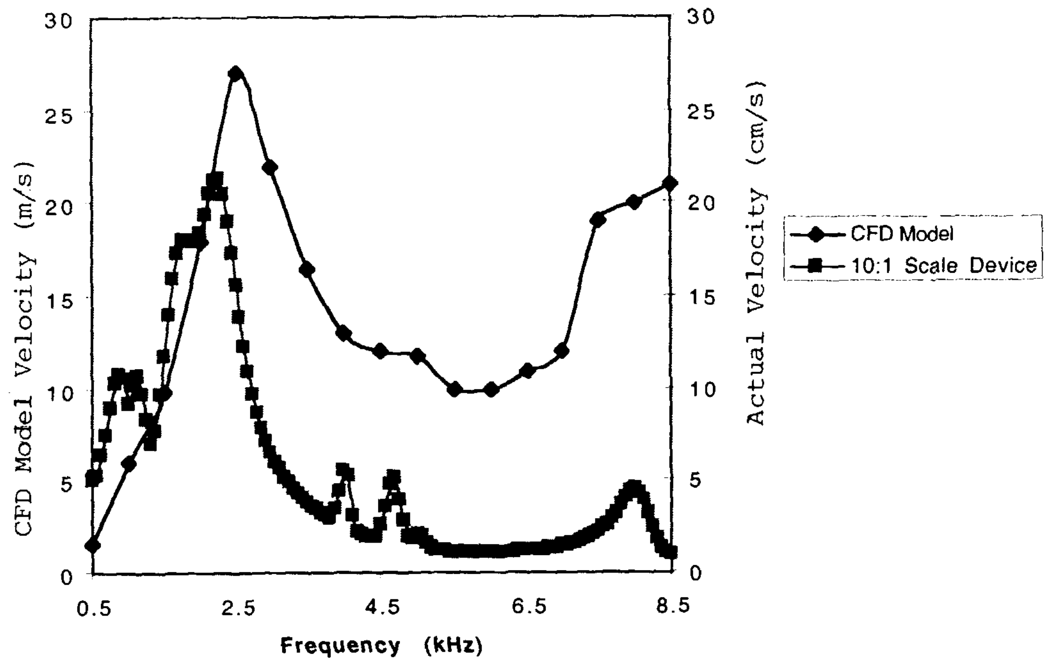

Figure 8: Predicted and measured velocities from the CFD and 10:1 geometrically scaled experiment. The CFD simulation assumed that membrane motion was +/- 30 μm. However the peak deformation in this experiment was +/- 1 μm.

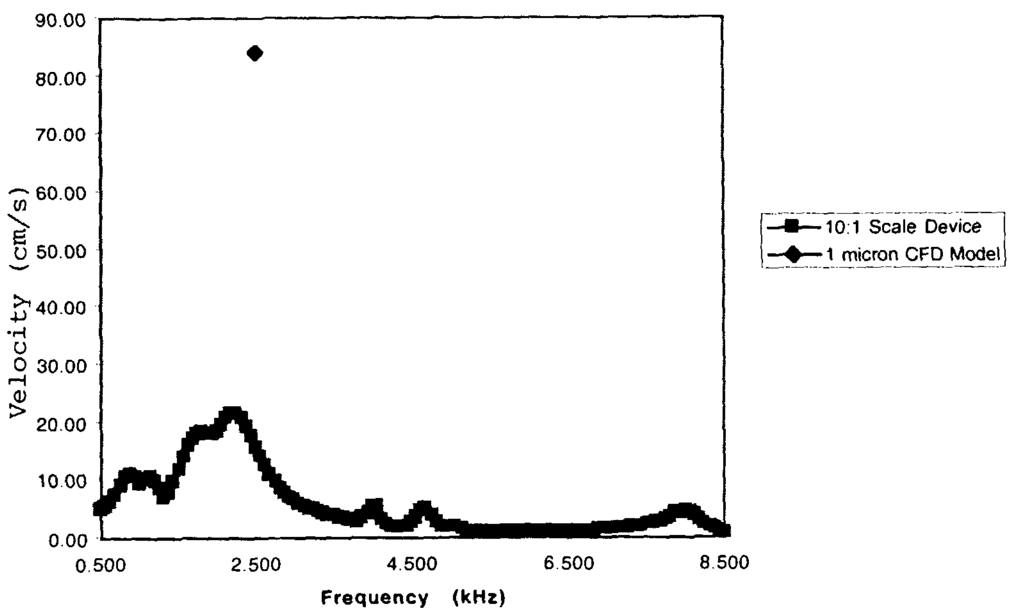

Figure 9: Predicted and measured velocities. Here the CFD simulation was re-evaluated to have +/- 1 μm deformation.

Unlike figure 8 where it was necessary to plot the simulation and experiment on two different scales, this graph has a single vertical scale. The measured and predicted performance differ by about a factor of four. Thus the magnitude of the membrane deformation is not the only unresolved issue.

SUMMARY AND CONCLUSIONS

A series of acoustic resonators combined along the periphery of an ejector shroud could theoretically provide thrust for a MEMS fabricated Micro Air Vehicle. A numerical model that simulates the internal flow of such a resonator has been developed. The computational model has an accompanying experimental model built for validation and calibration purposes.

To date the frequencies of the resonator appear to be simulated by the numerical model. In addition the general trends in the flow velocity as a function of frequency are predicted as well. However there is a large discrepancy between the predicted and measured flow velocities. These discrepancies are partially due to material and fabrication challenges in the construction of the experimental apparatus.

[1] INGARD, U. AND LABATE, S. 1950 Acoustic Circulation Effects and the Nonlinear Impedance of Orifices. *The Journal of the Acoustical Society of America.* **22**, 211-218.

[2] PARVIZ, B.A., BERNAL, L.P., AND NAJAFI, K. 1999 A Micromachined Helmholtz Resonator for Generation of Microjet Flows. *Proceedings of Transducers*

[3] MIHORA, D. J., AND REDMOND, P.J. 1980 ELECTROSTATICALLY FORMED ANTENNAS, *J. SPACECRAFT, VOL. 17, NO. 5, PG 465 - 473*

[4] Müller, M.O., BERNAL, L.P., MORAN, R.P., WASHABAUGH, P.D., PARVIZ, B.A., AND NAJAFI, K., 2000 Micromachines Acoustic Resonators for Microject Propulsion. *AIAA 38th Aerospace Science Conference, January 10-13, Reno Nevada,* **AIAA-2000-0547**

[5] FLUENT INCORPORATED, 1998 FLUENT USER'S GUIDE, RELEASE 4.5, *LEBANON, NH.*

[6] HALLIDAY, D., RESNICK, R., AND WALKER, J., 1993 FUNDAMENTALS OF PHYSICS: SOURCES OF SOUNDS, PG. 514-516, *WILEY AND SONS.*